Coherently induced stop-bands in resonantly absorbing and inhomogeneously broadened doped crystals

Qiong-Yi He,[1,2] Yan Xue,[1,2] M. Artoni,[3,4,*] G. C. La Rocca,[5,†] Ji-Hua Xu,[6] and Jin-Yue Gao[1,2,‡]
[1]*College of Physics, Jilin University, Changchun 130023, People's Republic of China*
[2]*Key Lab of Coherent Light, Atomic and Molecular Spectroscopy, Educational Ministry of China, Changchun, People's Republic of China*
[3]*Department of Chemistry and Physics of Materials, University of Brescia, Italy*
[4]*European Laboratory for Non-Linear Spectroscopy, Sesto Fiorentino (Firenze), Italy*
[5]*Scuola Normale Superiore and CNISM, 56100 Pisa, Italy*
[6]*Scuola Normale Superiore, Pisa, Italy*
(Received 25 November 2005; revised manuscript received 21 March 2006; published 30 May 2006)

Inhomogeneously broadened doped solids supporting electromagnetically induced transparency are viable materials where optically tunable photonic band gaps may be observed and results are shown for Pr:YSO and nitrogen-vacancy color center materials. Such crystals, when coherently driven by a strong pump beam in a suitably designed standing wave configuration, exhibit a tunable stop-band with rather different values of the reflectivity. The different propagating behavior is investigated and characterized for a weak probe across the gap region of the two materials.

DOI: 10.1103/PhysRevB.73.195124 PACS number(s): 42.70.Qs, 42.50.Gy, 03.75.Pp, 42.30.Rx

I. INTRODUCTION

Photonic crystals are inhomogeneous material media exhibiting periodic variations in space of their refractive index on length scales comparable to optical wavelengths. The periodic variation in their optical response leads to Bragg scattering of light, and electromagnetic wave propagation becomes best described in terms of a photonic band structure, akin to the electronic band structure in a crystalline solid.[1] In particular, when the light wave vector is close to the Brillouin zone boundary the propagation of light is strongly affected, leading to the existence of a range of frequencies, known as a photonic band gap, for which light does not propagate. The specific spatial dependence of the optical response in typical photonic crystals and the corresponding photonic band structure are determined once and for all by the way the material periodic structure is grown. Although a serious effort has been devoted over the past 10 years to microfabricate photonic band-gap materials, it is only recently that a clear route to synthesizing large-scale one, two, and three-dimensional band-gap materials with submicron lattice constants has been demonstrated using self-assembly methods.[2]

For many applications, however, it would be beneficial to obtain some degree of tunability of the photonic band structure. The possibility to tune the photonic band structure directly by optical means instead of having a photonic band structure determined once and for all at the growth stage would certainly be of great interest. Most familiar schemes to modify the optical properties of photonic crystals have relied on *slow* electro- and thermo-optics effects in infiltrated liquid crystals,[3] or on *fast* resonant and nonresonant optical effects in semiconductors.[4] Both effects enable one to tune the band-edge position, the Brillouin zone and the gross features of the photonic bands essentially being determined by the medium periodic structure.

Recently, however, there has been a considerable interest in generating photonic band-gap materials using nonlinear optical processes that arise from coherent quantum control of light-matter interactions. This is an altogether new approach toward tunable photonic crystals and requires the use of induced transparency in the presence of a standing wave optical potential.[5,6] Transparency may originate, e.g., from quantum interference effects taking place in multilevel systems, the simplest of which is a three-level atom in the Λ configuration driven by a monochromatic *traveling* light wave. This is commonly used to observe electromagnetically induced transparency[7] and the relevant dressed dielectric function experienced by a weak incident probe beam does not vary in space. Yet, when the same three-level atom is driven by a *standing* light wave,[8] the probe optical response is modulated periodically in space. This realizes a photonic band-gap material where the underlying medium is homogeneous, the photonic band structure being fully determined, rather than modified, by the external control beams that form the optical potential. Such optical lattices have been used to reversibly convert a light pulse into a stationary excitation inside a dilute volume of atoms.[9] An electromagnetically induced photonic band-gap material has also been devised in a semiconductor heterostructure with layers periodically doped with different atomic densities. The nonlinear optical excitations of these atoms creates a periodic refractive index contrast that leads to a photonic band gap.[10]

Apart from a few exceptions, most of the experiments carried out so far have dealt with atomic media. For many potential applications, however, solid-state media are preferred due to obvious advantages such as high atomic densities, compactness, absence of atomic diffusion, simplicity, and scalability during assembling. On the other hand, well-known difficulties with solid materials are typically very broad optical lines and fast decay of any coherence, which makes effects associated with quantum coherence and interference rather difficult to observe. Yet, electromagnetically induced transparency in solids has been attained in a class of materials exhibiting defect states such as, e.g., rare-earth impurities[11] or color center states.[12]

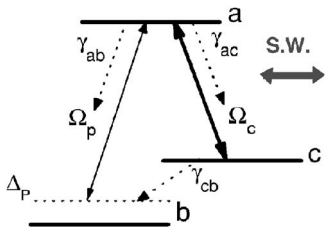

FIG. 1. Three-level Λ model for electromagnetically induced transparency. The probe (signal) field is nearly resonant with the transition from the ground to the excited state ($|a\rangle$), and the control fields (standing wave) is tuned to resonance between the $|c\rangle$ and the excited state.

In view of this, it would be interesting to investigate the possibility of photonic band-gap formation and control through all-optically induced resonant nonlinearities in multilevel solid systems that exhibit electromagnetically induced transparency. This is precisely what is done in this paper by examining the generation of one-dimensional photonic band-gap materials built from doped solids that support electromagnetically induced transparency. Solids with rare-earth impurities[11] or color center states[12] will be specifically examined. In both materials resonant absorption and inhomogeneous broadening play quite a significant role.[13] Yet, we will show that in both cases one can overcome the detrimental effect of dissipation[14] at the nodes of the external standing wave optical potential. Inhomogeneous broadening, on the other hand, does not always hamper band-gap formation, and in one of the two cases addressed here fairly large values of band-gap reflectivities still may be observed.

II. THEORETICAL MODEL

We consider here an inhomogeneously broadened doped solid supporting electromagnetically induced transparency which can be described by the simplified three-level Λ configuration shown in Fig. 1.[11–13] A weak *probe* beam, the reflection and transmission of which are the physical quantities we are interested in, having frequency ω_p and electric field amplitude E_p (i.e., Rabi frequency $\Omega_p=\mu_{ab}E_p/2\hbar$) propagates in the x direction in the presence of a strong *pump* or coupling beam of frequency ω_c and Rabi frequency Ω_c. The ground ($|b\rangle$), excited ($|a\rangle$), and metastable ($|c\rangle$) levels are such that the transitions $b-a$ (with transition matrix element μ_{ab}) and $c-a$ are nearly resonant with the probe and on resonance with the pump beams, respectively, while the excited level remains essentially empty. Our results will later be illustrated for a suitable choice of parameters appropriate to the cases of Pr:YSO and nitrogen-vacancy (NV) color center crystals, possibly with an additional repumper beam.[11–13]

Based on the semiclassical theory, using the standard density matrix formalism with the dipole approximation and the rotating wave approximation, the interaction Hamiltonian H_I for this system is

$$\mathbf{H}_I = -\hbar\mathbf{\Omega}_p\mathbf{e}^{-i\omega_p t}|\mathbf{a}\rangle\langle\mathbf{b}| - \hbar\mathbf{\Omega}_c\mathbf{e}^{-i\omega_c t}|\mathbf{a}\rangle\langle\mathbf{c}| + \mathbf{H.c.} \quad (1)$$

Including relaxation terms for this closed system as usual, the equations of motion for the density matrix in the interaction picture are (here the Rabi frequencies are assumed to be real, and $\hbar=1$)

$$\dot{\rho}_{aa} = -(\Gamma_{ab}+\Gamma_{ac})\rho_{aa} - i\Omega_p(\rho_{ab}-\rho_{ba}) - i\Omega_c(\rho_{ac}-\rho_{ca}),$$

$$\dot{\rho}_{bb} = \Gamma_{ab}\rho_{aa} + \Gamma_{cb}\rho_{cc} - \Gamma_{bc}\rho_{bb} + i\Omega_p(\rho_{ab}-\rho_{ba}),$$

$$\dot{\rho}_{cc} = \Gamma_{ac}\rho_{aa} - \Gamma_{cb}\rho_{cc} + \Gamma_{bc}\rho_{bb} + i\Omega_c(\rho_{ac}-\rho_{ca}),$$

$$\dot{\rho}_{ab} = -(i\Delta_{ab}+\gamma_{ab})\rho_{ab} - i\Omega_p(\rho_{aa}-\rho_{bb}) + i\Omega_c\rho_{cb},$$

$$\dot{\rho}_{cb} = -(i\Delta_{cb}+\gamma_{cb})\rho_{cb} - i\Omega_p\rho_{ca} + i\Omega_c\rho_{ab},$$

$$\dot{\rho}_{ac} = -(i\Delta_{ac}+\gamma_{ac})\rho_{ac} + i\Omega_p\rho_{bc} - i\Omega_c(\rho_{aa}-\rho_{cc}),$$

$$\rho_{aa}+\rho_{bb}+\rho_{cc} = 1, \quad (2)$$

where Γ_{ij} $(i,j=a,b,c)$ are the population relaxation rates, and the coherence decay rates for ρ_{ab}, ρ_{ac}, and ρ_{cb} are denoted by γ_{ab}, γ_{ac}, and γ_{cb}, respectively. We take $\Gamma_{cb}=\Gamma_{bc}$ so that before the action of the driving fields the levels $|b\rangle$ and $|c\rangle$ are equally populated We also assume $\Gamma_{ab}=\Gamma_{ac}$, $\gamma_{ab}=\gamma_{ac}$, and typical experimental parameters are given in Table I.[15] The Δ_{ij}'s are given by $\Delta_{ab}=\omega_{ab}-\omega_p=\Delta_p+\Delta\omega_{ab}$, $\Delta_{ac}=\omega_{ac}-\omega_c=\Delta\omega_{ac}$, $\Delta_{cb}=\omega_{cb}-\omega_p+\omega_c=\Delta_p+\Delta\omega_{cb}$, and $\Delta\omega_{ac}=\Delta\omega_{ab}-\Delta\omega_{cb}$. Here, ω_{ij} are the frequencies of the corresponding transitions, $\Delta\omega_{ij}$ represents the detuning of the center of the inhomogeneously broadened line from the transition frequency of a specific single ion within the inhomogeneous distribution, and the detuning of the probe field with respect to the line center of the $b-a$ transition is denoted by Δ_p and the coherent driving field is assumed to be exactly resonant.[13] Following the usual approach,[16] the presence of the pump field is treated to all orders, while the steady-state solution ρ_{ab} is found to first order, from which the dressed susceptibility seen by the probe is obtained.[17]

However, the analysis above yields the relevant equations for a single ion with specific detunings $\Delta\omega_{ab}$ and $\Delta\omega_{cb}$ determined by its position within its host. In order to obtain the relevant macroscopic susceptibility χ, such result is to be averaged over the entire frequency range of the corresponding transitions, as determined by the inhomogeneous broadening of the impurity lines in the host solid. We hereafter follow the treatment of Ref. 13, assuming that the inhomogeneous broadening could be described by a Lorentzian of appropriate width, and obtain[18]

$$\chi(\omega) = \int d\omega_{ab} f(\omega_{ab}) \int d\omega_{cb} f(\omega_{cb}) \frac{n\mu_{ab}^2}{2\hbar}\frac{\rho_{ab}}{\Omega_p}, \quad (3)$$

$$f(\omega_{ab(cb)}) = \frac{W^{ab(cb)}/\pi}{(\Delta\omega_{ab(cb)})^2 + (W^{ab(cb)})^2}, \quad (4)$$

where the $\Delta\omega_{ij}$'s are as in Eqs. (2), W^{ab}, W^{cb} are the inhomogeneous widths of the $|a\rangle\rightarrow|b\rangle$ and the $|c\rangle\rightarrow|b\rangle$ transitions, respectively, and n is the number of optically relevant impurities per unit volume. Finally, the dressed dielectric function experienced by the probe can be written as

$$\varepsilon(\omega) = n^2(\omega) = 1 + 4\pi\chi(\omega). \quad (5)$$

TABLE I. Relevant experimental parameters for rare-earth doped crystal (Pr:YSO) and for nitrogen-vacancy (NV) color centers in diamond (or NV diamond) (Refs. 20 and 21).

	W^{ab} (GHz)	W^{cb} (kHz)	Γ_{ab} (kHz)	γ_{ab} (kHz)	Γ_{cb} (Hz)	γ_{cb} (kHz)	λ (nm)	f	n (cm^{-3})
Pr:YSO	10^{-3}	30	6.1	9.0	0.01	2	605.7	3×10^{-7}	1.17×10^{15}
NV diamond	375	2.5×10^{3}	2.5×10^{4}	5×10^{4}	1	25	637	0.1	3×10^{18}

Unlike in typical lambda configurations leading to electromagnetically induced transparency where a continuous wave (cw) pump beam is used, the pump is here retroreflected upon impinging on a mirror of reflectivity R_m forming a standing wave (sw) pattern within the sample. The resulting pump Rabi frequency varies periodically along x,

$$\frac{\Omega_c^2(x)}{\Omega_o^2} = (1+\sqrt{R_m})^2\cos^2\left(\frac{\omega_c}{c}x\right) + (1-\sqrt{R_m})^2\sin^2\left(\frac{\omega_c}{c}x\right), \tag{6}$$

with a spatial periodicity a which is half the pump beam wavelength λ_c. For a perfect ($R_m=1$) standing wave $\Omega_c^2(x)$ varies periodically between 0 and $4\Omega_o^2$ and vanishes at the nodal positions where the medium remains absorbing. By slightly reducing the mirror reflectivity the pump intensity can however become nowhere vanishing, and the nodes will be replaced by quasinodes. In terms of the parameter $\eta=(1-\sqrt{R_m})/(1+\sqrt{R_m})$, where $0\leqslant\eta\ll1$, the minimum value of $\Omega_c^2(x)$ at a quasinode is approximately $4\eta^2\Omega_o^2$. The strong pump intensity pattern modifies in a periodic fashion the probe absorption and dispersion as one moves along x from quasinodes to antinodes. In particular, at the quasinodes nearly complete suppression of the probe absorption with a concomitant steep dispersion occurs within a narrow window centered around the $b-a$ transition frequency. At the antinodes, instead, the Autler-Townes splitting is so large that the dielectric function is nearly exactly unity within the narrow frequency range where the photonic band gap develop.[14]

Owing to the spatially periodic modulation induced by the pump (6), a probe with frequency $\omega_p\simeq\omega_{ab}$ propagates as in a one-dimensional photonic crystal with periodicity $a=\lambda_c/2$, where λ_c is approximately equal to the probe resonant transition wavelength λ_{ab}. The opening of a photonic stop band can be anticipated to occur at the Brillouin zone boundary π/a. A first step in characterizing the structure of the stop-band can be taken by numerically calculating the 2×2 unimodular transfer matrix[19] $M(\omega)$ representing the propagating through a single period of length a. Then, the translational invariance of the periodic medium is fulfilled by imposing the Bloch condition[1] on the photonic eigenstates,

$$\begin{pmatrix} E^+(x+a) \\ E^-(x+a) \end{pmatrix} = M(\omega)\begin{pmatrix} E^+(x) \\ E^-(x) \end{pmatrix} = \begin{pmatrix} e^{i\kappa a}E^+(x) \\ e^{i\kappa a}E^-(x) \end{pmatrix}, \tag{7}$$

where E^+ and E^- are the electric field amplitudes of the forward and backward (Bragg reflected) propagating probe, respectively, and $\kappa=\kappa'+i\kappa''$ is the Bloch complex wave vector of the corresponding probe photonic state. The one-dimensional photonic band structure is obtained from the solution of the corresponding determinantal equation $e^{2i\kappa a}-\mathrm{Tr}[M(\omega)]e^{i\kappa a}+1=0$ ($\det M=1$) and, noting that if κ is a solution $-\kappa$ is also a solution, one simply has

$$\kappa a = \pm\cos^{-1}\left[\frac{\mathrm{Tr}[M(\omega)]}{2}\right]. \tag{8}$$

The photonic band structure just discussed refers to Bloch modes for a probe in an infinite periodic stack, yet typical experiments[2,9] focus on propagation through samples of finite length. To calculate the corresponding reflectivity and transmissivity spectra, it is necessary to consider a finite sample of thickness $L=Na$ (typically with $N\gg1$), where N is the number of the standing wave periods. The total transfer matrix $M_{(N)}$ of a sample of thickness $L=Na$ ($N\gg1$) is simply given in terms of the single period transfer matrix M as $M_{(N)}=M^N$. Because M is unimodular, the following closed expression for $M_{(N)}$ holds true:

$$M_{(N)} = \frac{\sin(N\kappa a)}{\sin(\kappa a)}M - \frac{\sin[(N-1)\kappa a]}{\sin(\kappa a)}I, \tag{9}$$

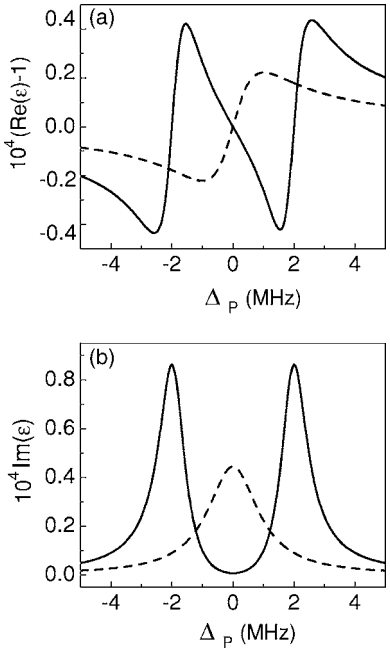

FIG. 2. Real (a) and imaginary (b) part of the dressed dielectric function for Pr:YSO when $\Omega_0=1$ MHz (solid lines) and $\Omega_0=0$ MHz (dashed lines), i.e., at the antinodes and at the nodes of the pump profile.

where I is the unity matrix. Such a compact expression enables one to write the reflection (R_N) and transmission (T_N) amplitudes for the L length in terms of the complex Bloch wave vector κ and the elements M_{ij} of the matrix M, namely,

$$R_N = \frac{M_{N(12)}}{M_{N(22)}} = \frac{M_{12}\sin(N\kappa a)}{M_{22}\sin(N\kappa a) - \sin[(N-1)\kappa a]}, \quad (10)$$

$$T_N = \frac{1}{M_{N(22)}} = \frac{\sin(\kappa a)}{M_{22}\sin(N\kappa a) - \sin[(N-1)\kappa a]}, \quad (11)$$

from which, in turn, the reflectivity, transmissivity, and absorption can be readily found by calculating respectively $|R_N|^2$, $|T_N|^2$, and $A = 1 - |R_N|^2 - |T_N|^2$.

III. RESULTS AND DISCUSSION

We report in the following our results for two different cases of experimental interest,[11–13,20,21] namely, for rare-earth doped crystals (Pr^{3+}-doped Y_2SiO_5 or Pr:YSO), and for nitrogen-vacancy (NV) color centers in diamond (or NV diamond). Electromagnetically induced transparency has been already observed in both materials[20,21] and all relevant experimental parameters are now listed in Table I below.

A. Pr:YSO

Because of its large ratio of inhomogeneous to homogeneous widths and long optical pumping lifetime, Pr:YSO is known as a good material for optical data storage. The crystal has also been used successfully in experiments involving electromagnetically induced transparency. The nominal density 4.7×10^{18} cm^{-3} of Pr ions in this crystal can be calculated straightforwardly from the crystal structure. The relevant optical transition at 605.7 nm has an inhomogeneous width $W^{ab} \simeq 2$ GHz, while the inhomogeneous width of the spin transition is $W^{cb} \simeq 30$ kHz. In the experiment of Ref. 21, the inhomogeneous broadening of the optical transition is reduced to the magnitude of the laser beam jitter ($\Delta\nu_{jit} = 1$ MHz) using an optical repumper scheme, at the price of reducing the effective density of Pr ions to 1.17×10^{15} cm^{-3}.

Typical profiles of the real and imaginary parts of the dressed dielectric function can be obtained by numerical evaluation of Eqs. (3)–(5), and we show in Fig. 2 the case of

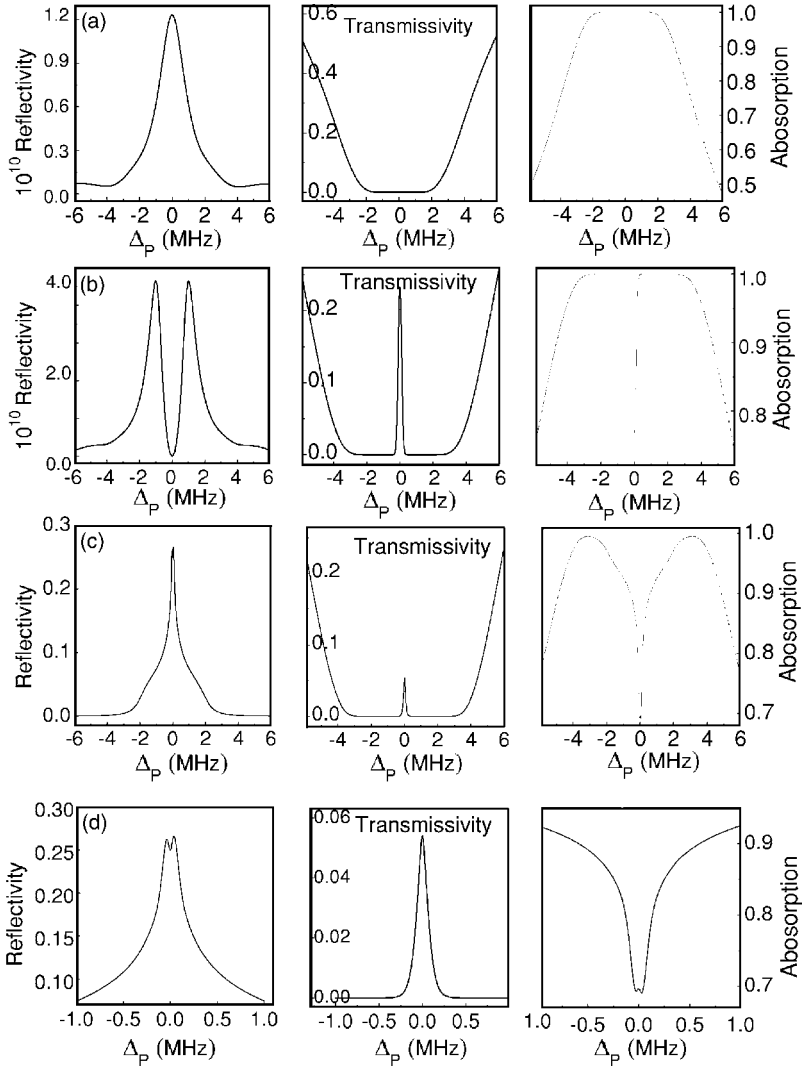

FIG. 3. Reflectivity, transmission, and absorption spectra for a 5 cm long sample of Pr:YSO when (a) no pump is on and, respectively, when (b) a CW pump and (c) a modified SW pump with $\eta=0$ and $\alpha=0.98$ mrad is on. In all cases the pump has the same intensity $\Omega_0=1$ MHz. (d) represents the reflectivity, transmittivity, and absorption profiles at small detuning range.

Pr:YSO as a function of the probe detuning in the absence (dashed lines) and in the presence of a resonant coupling field (solid lines). Here, assuming that the intensity of the coupling field corresponds to the peak intensity of a perfect standing wave ($\eta=0$), the dashed and solid lines show the response that the probe field experiences at the nodes and at the antinodes, respectively.

Equations (9)–(11) are the basis of the subsequent discussion of Fig. 3, in which the reflectivity, transmission, and absorption spectra are shown when (a) no pump; (b) a cw pump; and (c), (d) sw pump, respectively, are used. Considerably larger reflectivities, as in (c), are instead obtained using a configuration[14] in which the forward and backward control beams are slightly misaligned by an angle α. The spatial periodicity in this case is given by $(\lambda_c/2)/\cos(\alpha/2)$. By comparing the three results, it appears that one attains an appreciable band-gap reflectivity when pumping in a standing wave configuration occurs.

When we instead increase the Rabi frequency to $\Omega_0=10$ MHz and unbalance the standing wave potential ($\eta=0.05$), yet keep the same misalignment ($\alpha=0.98$ mrad), a well-developed band gap characterized by $\kappa' \simeq \pi/a$ and $\kappa'' \neq 0$ appears as shown in Fig. 4, which is derived from the real and imaginary parts of the Bloch complex wave vector [Eq. (8)]. Within the gap, $\kappa'' \neq 0$ corresponds to reflection rather than absorption of the probe, although κ'' is not large enough to stop the probe within a sample a few centimeters long.

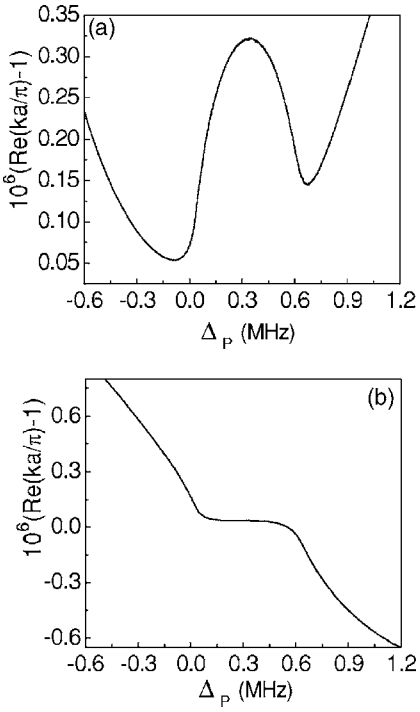

FIG. 4. Photonic band-gap structure near the Brillouin zone boundary in Pr:YSO when $\Omega_0=10$ MHz, $\eta=0.05$, and $\alpha=0.98$ mrad. The upper (a) and lower (b) frames denote, respectively, the imaginary and real parts of the Bloch wave vector.

B. NV color centers

The main drawback of Pr:YSO is, however, the weak optical oscillator strength ($\sim 10^{-7}$), common to many other spectral hole-burning materials. For this reason, we investigate the alternative case of NV color centers in diamond having a much larger optical oscillator strength (~ 0.1). Like Pr:YSO, this has been successful to observe electromagnetically induced transparency.

In Fig. 5, the typical profiles of the real and imaginary parts of the dressed dielectric function of nitrogen-vacancy (NV) color centers in diamond are shown as a function of the probe detuning Δ_p in the absence of the coupling field (dashed lines) and in the presence of a strong resonant coupling field $\Omega_0=20$ GHz (solid lines). Figure 6 shows the reflectivity spectra of NV diamond when respectively (a) no pump and (b) a modified standing wave pump is on. It is clear that without the pump, the reflectivity is very low and the solid medium is completely opaque to the signal near resonance. The peak of the reflected beam becomes however a substantial fraction of the input signal beam, and much larger than in the case of Pr:YSO above, when a standing wave coherent driving pump is on. In both cases the transmittivity is extremely small and is not reported here. Furthermore, when a continuous wave (cw) pump is present we can show that the reflectivity becomes even smaller than in (a) while the transmission exhibits a very small peak due to the usual electromagnetically induced transparency. Both values of the reflectivity and transmittivity are however basically vanishing and will not be reported here either. The incipient photonic band-gap structure around the lowest photonic gap corresponding to the case of Fig. 6(b) is reported instead in Fig. 7.

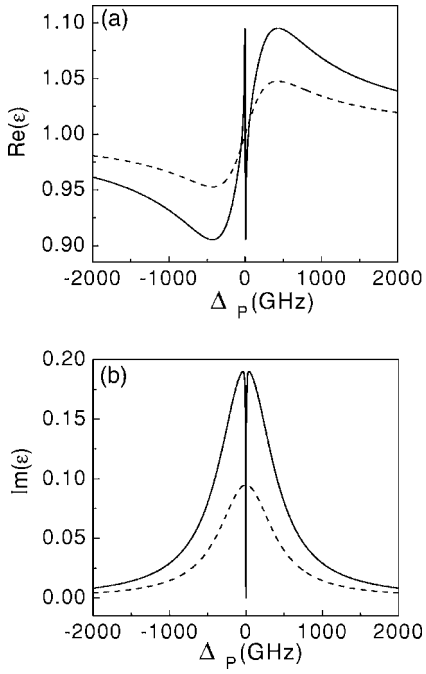

FIG. 5. Real (a) and imaginary (b) parts of the dressed dielectric function for NV diamond when $\Omega_0=20$ GHz (solid lines) and $\Omega_0=0$ GHz (dashed lines), i.e., to the antinodes and to the nodes of the pump profile.

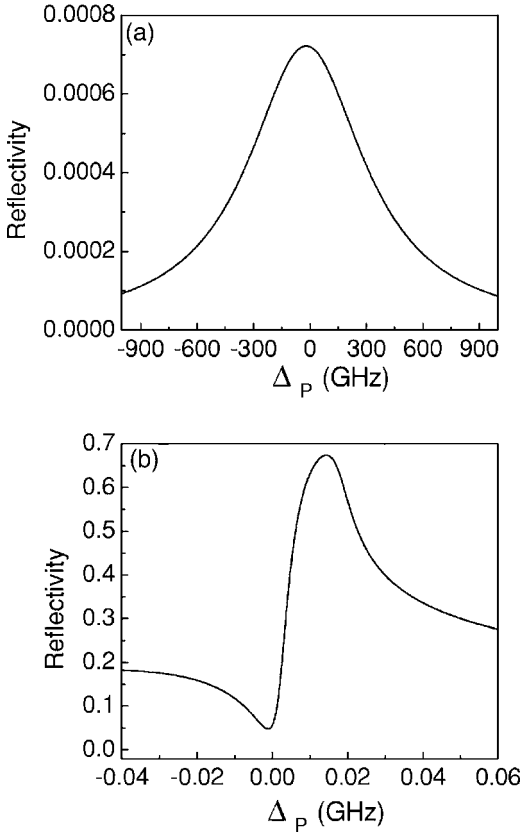

FIG. 6. Reflectivity spectra for a 2 cm long sample of NV diamond when (a) No pump is on and (b) a modified SW pump with $\eta=0.1$ and $\alpha=89.4$ mrad is on. Here, the pump intensity is $\Omega_0=20$ GHz.

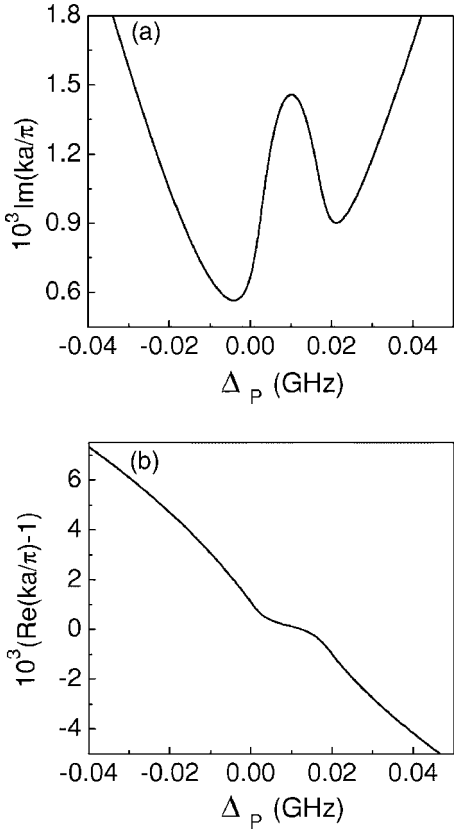

FIG. 7. Probe photonic band-gap structure near the Brillouin zone boundary in NV diamond when $\Omega_0=20$ GHz, $\eta=0.1$, and $\alpha=89.4$ mrad. As in Fig. 4 the upper (a) and lower (b) frames denote, respectively, the imaginary and real parts of the Bloch wave vector.

IV. CONCLUSIONS

Photonic stop-bands in one-dimensional materials with defects states and where electromagnetically induced transparency takes place may be observed in principle. Solids with rare-earth impurities and color center states have been specifically studied here. While a careful design of the external driving optical potential prevents absorption from spoiling the gap structure in both cases, inhomogeneous broadening affects the gap formation in a different way in the two different samples. Our results show, however, that optically tunable high-reflectivity stop-bands may be achieved, though with rather large Rabi frequencies and sufficiently long samples. In general, the position and the width of the stop band can be tuned by changing the standing wave configuration (η,α) and the control beam Rabi frequency Ω_0. Although we have chosen well-known experimental cases, other inhomogeneously broadened doped solid amenable[13,22] to the observation of electromagnetically induced transparency may be employed. Using a higher number of control beams, 2D and 3D configurations[23] can similarly be realized exhibiting photonic stop-bands along different directions of the Brillouin zone and which might turn out to be useful for multiple beam applications. Finally, tunable photonic structures such as those we study here may possibly be sought after as a promising avenue, e.g., toward deterministic photon-photon entanglement[24] or the enhancement of nonlinear interactions between weak light pulses.[25]

ACKNOWLEDGMENTS

The authors acknowledge financial support from the NSFC (Grant No. 10334010), the Graduate Innovation Lab of Jilin University, MAE (Grant ST China-Italy), and MIUR (Accion Integrada IT-1603). Qiong-Yi He is grateful for the hospitality at the Scuola Normale Superiore in Pisa.

*Electronic address: artoni@lens.unifi.it
†Electronic address: larocca@sns.it
‡Electronic address: jygao@mail.jlu.edu.cn

[1] F. Bassani and G. Pastori Parravicini, *Electronic States and Optical Transitions in Solids* (Pergamon, Oxford, 1975).
[2] S. Johnson, J. Joannopoulos, R. Meade, and J. Winn, *Photonic Crystals: The Road from Theory to Practice* (Kluwer, Norwell, 2002); R. Slusher and B. Eggleton, *Nonlinear Photonic Crystals*

(Springer, Berlin, 2003); D. S. Wiersma, R. Sapienza, S. Mujumdar, M. Colocci, M. Ghulinyan, and L. Pavesi, J. Opt. A, Pure Appl. Opt. **7**, 190 (2005).

[3] K. Busch and S. John, Phys. Rev. Lett. **83**, 967 (1999); D. Kang, J. E. Maclennan, N. A. Clark, A. A. Zakhidov, and R. H. Baughman, *ibid.* **86**, 4052 (2001).

[4] P. M. Johnson, A. F. Koenderink, and W. L. Vos, Phys. Rev. B **66**, 081102(R) (2002); H. W. Tan, H. M. van Driel, S. L. Schweizer, R. B. Wehrspohn, and U. Gosele, *ibid.* **70**, 205110 (2004).

[5] A. Andre and M. D. Lukin, Phys. Rev. Lett. **89**, 143602 (2002).

[6] H. Kang, G. Hernandez, and Y. Zhu, Phys. Rev. Lett. **93**, 073601 (2004).

[7] G. Alzetta, A. Gozzini, L. Moi, and G. Orriols, Nuovo Cimento Soc. Ital. Fis., A **36**, 5 (1976); S. Harris, Phys. Today **50**, 36 (1997); E. Arimondo, in *Progress in Optics XXXV*, edited by E. Wolf (Elsevier Science, Amsterdam, 1996), p. 257; A. B. Matsko, O. Kocharovskaya, Y. Rostovtsev, G. R. Welch, A. S. Zibrov, and M. A. Scully, Adv. At., Mol., Opt. Phys. **46**, 191 (2001).

[8] R. Corbalán, A. N. Pisarchik, V. N. Chizhevsky, and R. Vilaseca, Opt. Commun. **133**, 225 (1997); H. Y. Ling, Y. Q. Li, and M. Xiao, Phys. Rev. A **57**, 1338 (1998); M. Mitsunaga and N. Imoto, *ibid.* **59**, 4773 (1999); F. Silva, J. Mompart, V. Ahufinger, and R. Corbalán, *ibid.* **64**, 033802 (2001).

[9] M. Bajcsy, A. S. Zibrov, and M. D. Lukin, Nature (London) **426**, 638 (2003).

[10] Y. V. Rostovstev, A. B. Matsko, and M. O. Scully, Phys. Rev. A **57**, 4919 (1998).

[11] B. S. Ham, M. S. Shahriar, and R. P. Hemmer, Opt. Lett. **22**, 1138 (1997); K. Ichimura, K. Yamamoto, and N. Gemma, Phys. Rev. A **58**, 4116 (1998); A. V. Turukhin, V. S. Sudarshanam, M. S. Shahriar, J. A. Musser, B. S. Ham, and P. R. Hemmer; Phys. Rev. Lett. **88**, 023602 (2001).

[12] C. Wei and N. B. Manson, Phys. Rev. A **60**, 2540 (1999).

[13] E. Kuznetsova, O. Kocharovskaya, P. Hemmer, and M. O. Scully, Phys. Rev. A **66**, 063802 (2002).

[14] Absorption in general blurs the distinction between photonic bands and gaps and may even suppress it. A detailed treatment of resonantly absorbing photonic band-gap systems based on atoms is given in M. Artoni, G. La Rocca, and F. Bassani, Phys. Rev. E **72**, 046604 (2005); M. Artoni and G. La Rocca, Phys. Rev. Lett. **96**, 073905 (2006).

[15] We have checked that moderate variations of these parameters, in particular for the γ_{cb}, do not significantly change our results.

[16] See *Quantum Optics*, M. O. Scully and M. S. Zubairy (Cambridge University Press, Cambridge, 1997).

[17] In the systems considered here and in the frequency regions where the photonic gaps open up, local field effects on the dressed susceptibility due to dipole-dipole interactions can be safely neglected. See, e.g., I. V. Jyotsna and G. S. Agarwal, Phys. Rev. A **53**, 1690 (1996); G. S. Agarwal and Robert W. Boyd, *ibid.* **60**, R2681 (1999).

[18] The use of Lorentzian line shapes allows us to obtain analytical results for χ as described in detail in Ref. 13. Rather than reproducing those rather lengthy formulas here, we prefer to plot directly χ for the cases of our interest in Figs. 2 and 5.

[19] M. Born and E. Wolf, *Principles of Optics*, 6th ed. (Cambridge University Press, Cambridge, 1980).

[20] P. R. Hemmer, A. V. Turukhin, M. S. Shahriar, and J. Musser, Opt. Lett. **26**, 361 (2001).

[21] B. S. Ham, P. R. Hemmer, and M. S. Shahriar, Opt. Commun. **144**, 227 (1997); B. S. Ham, M. S. Shahriar, M. K. Kim, and P. R. Hemmer, Opt. Lett. **22**, 1849 (1997); J. J. Longdell, E. Fraval, M. J. Sellars, and N. B. Manson, Phys. Rev. Lett. **95**, 063601 (2005); E. Baldit, K. Bencheikh, P. Monnier, J. A. Levenson, and V. Rouget, *ibid.* **95**, 143601 (2005).

[22] M. Johnsson and K. Molmer, Phys. Rev. A **70**, 032320 (2004).

[23] C. S. Adams and E. Riis, Prog. Quantum Electron. **21**, 1 (1997).

[24] I. Friedler, G. Kurizki, and D. Petrosyan, Phys. Rev. A **71**, 023803 (2005).

[25] A. Andre, M. Bajcsy, A. S. Zibrov, and M. D. Lukin, Phys. Rev. Lett. **94**, 063902 (2005).